(12) Carman, C. J. *Macromolecules* **1973**, *6*, 725.
(13) Pham, Q. T.; Millan, J. L.; Madruga, E. L. *Makromol. Chem.* **1974**, *175*, 945.
(14) Lemstra, P. J.; Keller, A.; Cudby, M. *J. Polym. Sci., Polym. Phys. Ed.* **1978**, *16*, 1507.
(15) Fox, T. G.; Schnecko, H. W. *Polymer* **1962**, *3*, 575.
(16) Manson, J. A.; Iobst, S. A.; Acosta, R. *J. Macromol. Sci., Phys.* **1974**, *B9*, 301.
(17) Guerrero, S. J.; Keller, A.; Soni, P. L.; Geil, P. H. *J. Macromol. Sci., Phys.* **1981**, *B20*, 161.
(18) Guerrero, S. J.; Keller, A. *J. Macromol. Sci., Phys.* **1981**, *B20*, 167.
(19) Small, P. A. *J. Appl. Chem.* **1953**, *3*, 71.
(20) Kaltwasser, H.; Klose, W. *Plaste Kautsch.* **1966**, *13*, 583.
(21) Miller, R. L. *J. Polym. Sci.* **1962**, *57*, 975.
(22) Illers, K. H. *J. Macromol. Sci., Phys.* **1977**, *B14*, 471.
(23) Wunderlich, B. *J. Phys. Chem.* **1960**, *64*, 1052.
(24) Wunderlich, B.; Jones, L. D. *J. Macromol. Sci., Phys.* **1969**, *B3*, 67.
(25) Brown, D. W.; Wall, L. A. *J. Polym. Sci., Part A-2* **1969**, *7*, 601.
(26) Wong, K. C.; Chen, F. C.; Choy, C. L. *Polymer* **1975**, *16*, 85.
(27) Goldstein, M. *J. Chem. Phys.* **1977**, *67*, 2246.
(28) O'Reilley, J. M. *J. Appl. Phys.* **1977**, *48*, 4043.
(29) DiMarzio, E. A.; Dowell, F. *J. Appl. Phys.* **1979**, *50*, 6061.
(30) Roe, R. J.; Tonelli, A. E. *Macromolecules* **1979**, *128*, 878.
(31) Tanaka, N. *Polymer* **1979**, *20*, 593.
(32) Illers, K. H. *Makromol. Chem.* **1969**, *127*, 1.
(33) Grewer, T.; Wilski, H. *Kolloid Z. Z. Polym.* **1970**, *238*, 426 and references therein.
(34) Ceccorulli, G.; Pizzoli, M.; Pezzin, G. *J. Macromol. Sci., Phys.* **1977**, *B14*, 499.
(35) Guerrero, S. J.; Meader, D.; Keller, A. *J. Macromol. Sci., Phys.* **1981**, *B20*, 185.
(36) "Polymer Handbook"; Brandrup, J., Imerugt, E. H., Eds.; Wiley: New York, 1975; Chapter V-7.
(37) Gouinlock, E. V. *J. Polym. Sci., Phys. Ed.* **1975**, *13*, 1533.
(38) Koenig, J. L.; Antoon, M. K. *J. Polym. Sci., Phys. Ed.* **1977**, *15*, 1379.
(39) Bopp, R. C.; Gaur, U.; Kambour, R. P.; Wunderlich, B. *J. Therm. Anal.* **1982**, *25*, 243.
(40) Komoroski, R. A.; Mandelkern, L. "Applications of Polymer Spectroscopy"; Brame, E. G., Jr., Ed.; Academic Press: New York, 1978; p 57.
(41) Boyer, R. F. *Macromol. Sci., Phys.* **1973**, *B7*, 487.
(42) Wunderlich, B.; Gaur, V. *Pure Appl. Chem.* **1980**, *52*, 445.
(43) Chang, S. S. *J. Res. Natl. Bur. Stand. (U.S.)* **1977**, *82*, 9.

Extension of Thermal Field-Flow Fractionation to Ultrahigh (20×10^6) Molecular Weight Polystyrenes

Yu S. Gao, Karin D. Caldwell, Marcus N. Myers, and J. Calvin Giddings*

Department of Chemistry, University of Utah, Salt Lake City, Utah 84112.
Received July 10, 1984

ABSTRACT: The theory and practice of thermal field-flow fractionation (thermal FFF) as a tool for characterizing the molecular weight distribution of polymers are reviewed and a number of advantages with respect to size exclusion chromatography (SEC or GPC) are summarized. Retention values are measured and tabulated for linear polystyrenes in THF in the molecular weight range 5.1×10^4 to 20.6×10^6. For calibration purposes, it is shown that a plot of the logarithm of the product of retention parameter λ and temperature drop ΔT vs. the logarithm of molecular weight is linear for this entire experimental range with a slope of −0.53. To demonstrate fractionation and the absence of shear degradation in the higher molecular weight range, a fraction was cut from the 20.6M peak, reinjected, and observed to elute as a narrow peak centered near the position of the cut. Calculations based on nonequilibrium theory show that column band broadening for a 20.6M peak eluted at $\Delta T = 8$ °C contributes only about 10% to the plate height, the remainder arising from the fractionation of the molecular weight distribution. Thus a molecular weight distribution curve was obtained. We found the latter to be characterized by $M_w/M_n \cong 1.52$. We conclude that thermal FFF is applicable to ultrahigh molecular weight polymers but that other FFF subtechniques, especially flow FFF and sedimentation FFF, may also work in this molecular weight range.

Introduction

Field-flow fractionation (FFF) is a family of high-resolution techniques that has proven applicable to the analytical fractionation of a very wide range of aqueous and nonaqueous systems of macromolecules, colloidal particles, and even larger particles.[1-5] FFF is a flow-elution method, like chromatography, but differential retention is achieved by the application of an external field or gradient perpendicular to the narrow, ribbon-like flow channel. The most common fields and gradients are provided by centrifugation or gravity (sedimentation FFF), a liquid cross-flow (flow FFF), electrical fields (electrical FFF), and temperature gradients (thermal FFF). Each of these subtechniques has its own unique characteristics and applicability.

Thermal FFF has proven to be the most useful subtechnique for lipophilic polymers; the polymer molecular weight distribution can be obtained from the fractionation pattern.[6-8] Currently, most polymer molecular weight determinations are performed by size exclusion chromatography (SEC or GPC).[9] In SEC, the elution range is narrowly limited to values between the interstitial volume of the column and the total liquid volume. This confined range limits the number of components which can be resolved by a given column.[10] By contrast, with FFF there is no inherent limit to the elution volume range, allowing an increased number of resolvable peaks. In addition, the field strength in FFF can be varied between runs or within a run (programming) to provide maximum adaptability to sample type, in contrast to the rather rigid range of applicability of any given SEC column. Furthermore, the fractionating power of FFF is several times that of SEC for a given number of theoretical plates.[10]

For ultrahigh molecular weight polymers, SEC is also hampered by the shear degradation of polymer chains in the high-shear flow of the packed bed.[11-13] Since velocity gradients in the open FFF channel are perhaps an order of magnitude less than those in high-performance SEC columns, and since extensional shear is virtually absent, shear problems should be greatly reduced in FFF.

In our previous work, the relationship between sample molecular weight and thermal FFF retention was explored for a variety of different polymers, e.g., linear poly-

0024-9297/85/2218-1272$01.50/0

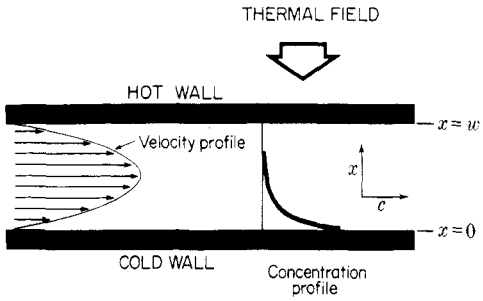

Figure 1. Principle of FFF operation. Coordinate x represents distance from the cold wall. The exponential sample concentration profile of eq 1 is indicated in the figure.

styrene,[14-17] polyethylene,[8] polyisoprene,[18] poly(tetrahydrofuran),[18] and poly(methyl methacrylate).[18,19] The linear polystyrene standards were also examined in a number of different solvents.[20] The universal trend is one of greater retention for increased molecular weight, although the level of retention for each sample varied with the solvent.

Despite extensive studies of the thermal FFF behavior of linear polystyrene samples, no systematic work has involved molecular weights above 160 000. (Separated peaks with molecular weights up to $\sim 8 \times 10^6$ have been produced by a programming method.[16]) In this study we extend the molecular weight range of carefully studied polymers by over 2 orders of magnitude, demonstrating retention and fractionation of samples with molecular weights up to 20.6×10^6. The relationships developed previously between retention and the molecular weight of linear polystyrenes in good solvents are examined for applicability over the greatly extended range of molecular weights studied here.

Theory

The basic retention mechanism in FFF has been described in numerous publications.[21,22] For the purpose of this study, we will concentrate on the features applicable to FFF separation under the influence of thermal gradients, i.e., on thermal FFF. The thermal FFF channel is a thin duct with a rectangular cross-section, having an aspect (breadth/thickness) ratio large enough (40–200) that the flow approximates that between infinite parallel plates. Across this channel a temperature gradient is applied, as illustrated in Figure 1. In such a gradient, polymer molecules are known to migrate toward the cold wall. This migration is governed by the thermal diffusivity D_T, which varies with temperature but is approximately independent of molecular weight.[20] The accumulation by thermal diffusion will be counteracted by ordinary molecular diffusion governed by diffusion coefficient D. A steady-state distribution of solute is achieved in minutes or less (the "relaxation" time); this distribution can be expressed in terms of the concentration c_0 at the cold wall and the distance x from this wall

$$c(x) = c_0 e^{-x/l} \tag{1}$$

where l is a measure of the thickness of the solute layer.

Introducing λ as the ratio of l to the thickness w of the channel, $\lambda = l/w$, we are able to express λ in terms of the ratio D/D_T[16]

$$\lambda = \frac{l}{w} = \frac{D}{D_T} \frac{1}{(dT/dx)w} \tag{2}$$

Equation 2 is based on the assumption that the thermal expansion of the solvent can be neglected.[23] The magnitude of the ratio D/D_T depends on the molecular weight of the polymer sample and on the nature of the carrier solvent. The molecular weight dependence arises mainly from the D term; we will assume the ratio to be described by a simple power law analogous to that commonly used to relate D and M[19]

$$D/D_T = A'M^{-b'} \tag{3}$$

The denominator in expression 2 contains the product of the temperature gradient dT/dx and the distance w across the channel. To a first approximation the gradient can be assumed linear, in which case dT/dx can be replaced by $\Delta T/w$, where ΔT is the temperature drop across the channel. This simplification, together with the expression for D/D_T given by eq 3, converts eq 2 into a more practical form for molecular weight evaluation

$$\lambda \simeq A'M^{-b'}/\Delta T \tag{4}$$

or, in logarithmic form

$$\log \lambda = -b' \log M + \log A' - \log \Delta T \tag{5}$$

or, with λ and ΔT terms grouped together

$$\log (\lambda \Delta T) = -b' \log M + \log A' \tag{6}$$

The linear relationships expressed by eq 5 and 6 are useful for the graphical analysis of experimental data.

Equations 4–6 show that sample constituents of different molecular weight will form layers of different reduced thickness λ in the cold wall region of the channel. When the carrier liquid is forced to flow down the channel, the different polymer constituents are carried downstream at velocities which depend on their degree of extension out from the wall into faster flow lines, an extension measured by λ. The *retention ratio* R *for a given component* is defined as the zone velocity divided by the average velocity of the carrier. This parameter is determined experimentally as the ratio of the channel volume V^0 to the observed elution volume V_r for the component zone. For most forms of FFF (excluding thermal FFF), which operate under isothermal conditions, R can be expressed as a simple function of λ[21]

$$R = V^0/V_r = 6\lambda[\coth (1/2\lambda) - 2\lambda] \tag{7}$$

with the limiting form

$$R = 6\lambda \tag{8}$$

obeyed for small values of λ. In the presence of a temperature gradient, there is a gradient in viscosity across the channel which gives rise to a skewed velocity profile. The correction for the departure from isoviscous flow is somewhat involved[25] and will not be reported here. Its effect on the relationship between R and λ is illustrated in Figure 2 for a ΔT of 41 °C. For temperature differences of less than 10 °C, the correction is negligible.

Through eq 7 and its viscosity-corrected analogue, it is possible to obtain λ from the observed elution volume V_r. According to eq 4–6, λ can be used to obtain sample molecular weight M provided constants A' and b' have been established.

Any chromatographic-like process gives rise to the broadening of sample zones as they migrate through the column. In the case of FFF, this zone broadening, expressed in terms of plate height H, depends on the level of retention (through λ), the average velocity of carrier flow $\langle v \rangle$, and the sample's diffusivity D and polydispersity μ in the following manner[26]

$$H = \chi(\lambda)\frac{w^2}{D}\langle v \rangle + L\left(\frac{d \ln V_r}{d \ln M}\right)^2 \frac{\mu - 1}{\mu} \tag{9}$$

Here $\chi(\lambda)$ is the retention-dependent nonequilibrium

coefficient,[27] and w and L are the column's thickness and length, respectively. The derivative d ln V_r/d ln M is the mass selectivity of the system and μ is the ratio of weight- to number-average molecular weight $\bar{M}_w/\bar{M}_n$.

The second term of eq 9, arising in sample polydispersity, represents the broadening of the peak due to actual polymer fractionation. Because of the high selectivity of FFF, this term is the dominant peak-broadening term for polymers of all but the smallest μ's. With increasing μ, the fractionation represented by the polydispersity term becomes more clearly defined and the peak profile evolves into a molecular weight distribution profile. However, a scale correction factor[28] must be applied to transform the profile from the retention volume axis to the molecular weight axis, yielding a molecular weight distribution (MWD) curve.

If the MWD curve is represented by $m(M)$, then the mass of polymer falling between molecular weight M and $M + dM$, $m\,dM$, corresponds to the polymer mass eluting between retention volume V_r and $V_r + dV_r$; i.e.

$$m\,dM = c\,dV_r \tag{10}$$

where $c(V_r)$ is the concentration expressed as polymer mass/volume in the eluent, a quantity represented by the detector signal profile (the fractogram). Thus the unnormalized MWD curve $m(M)$ is obtained as

$$m(M) = c(V_r)\frac{dV_r}{dM} \tag{11}$$

which requires evaluation of the scale correction factor dV_r/dM.

The scale correction factor can be expressed as

$$\frac{dV_r}{dM} = \frac{dV_r}{dR}\frac{dR}{d\lambda}\frac{d\gamma}{dM} \tag{12}$$

where, from eq 7

$$\frac{dV_r}{dR} = -\frac{V_r}{R} \tag{13}$$

and

$$\frac{dR}{d\lambda} = \frac{3}{\lambda}\left[\frac{R^2}{36\lambda^2} + R - 1\right] \tag{14}$$

From eq 4

$$\frac{d\lambda}{dM} = -b\lambda M^{-1} \tag{15}$$

which gives eq 12 the following form:

$$\frac{dV_r}{dM} = -\frac{3V_r b'}{M}\left[\frac{R}{36\lambda^2} + 1 - \frac{1}{R}\right] \tag{16}$$

In the limit of high retention, where eq 8 becomes applicable, the scale correction factor reduces to the simple expression

$$\lim_{M\to\infty}\frac{dV_r}{dM} = \frac{b'V_r}{M} = \frac{b'\Delta T V^0}{6A'M^{1-b'}} \tag{17}$$

Experimental Section

The thermal FFF system was assembled from two highly polished, chrome-plated copper bars as described previously.[29] The upper bar is equipped with two 1.5-kW cartridge heaters whereas tap water is circulated through the lower bar for cooling. The two bars are sandwiched together around a 0.0254-cm-thick (dimension w) mylar sheet which acts as a spacer. From this sheet a 2.0-cm-wide channel with tapered ends has been cut (47.0 cm from tip to tip). The void volume V^0 equals 2.3 mL. The cold wall temperature was held at 13 °C, unless otherwise specified,

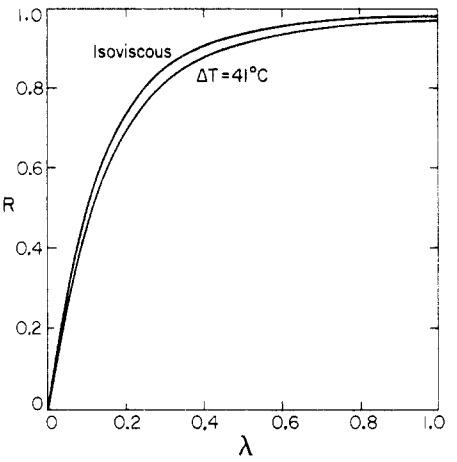

Figure 2. Relationship between the retention ratio R and the retention parameter λ (eq 2) for the carrier tetrahydrofuran at a cold wall temperature of 15 °C and a hot wall temperature of 56 °C. The upper curve, labeled "isoviscous", is obtained from eq 7 and is not corrected for the gradient in viscosity induced by the temperature differential. The lower curve, labeled "ΔT = 41 °C", is corrected according to ref 20.

Table I
Polystyrene Standards Employed in This Study

MW × 10^{-4}	polydispersity	source
5.10	1.009	Waters
9.70	1.009	Waters
16.0	1.009	Waters
30.0	1.06	Pressure Chemical Co.
41.1	1.10	Mann
49.8	1.20	Pressure Chemical Co.
60.0	1.10	Pressure Chemical Co.
67.0	1.15	Pressure Chemical Co.
86.0	1.15	Mann
180	<1.2	Mann
410	1.1	Duke
675	1.16	Polymer Laboratories
842	1.17	TSK
2060		TSK

and monitored continuously by means of a copper–constantan thermocouple.

Tetrahydrofuran (THF) (certified grade, Fisher Scientific) was used as a carrier; it was pumped through the system at a steady flow rate of 7.2 mL/h, which corresponds to a linear velocity of 0.0394 cm/s. To eliminate pulsing, the solvent was delivered by a pneumatic pump[17] consisting of a coiled tube with 600-mL volume which contained the THF. This tube was kept at a constant pressure by a stream of helium from a tank. A fine metering valve (Nupro SS-21 RS4) was used at the outlet of the coil to regulate the flow rate.

The polymer samples were all linear polystyrenes; the suppliers, assigned molecular weights, and polydispersities are listed in Table I. Sample concentrations were 1 mg/mL throughout this study. Injections of 1–20 μL were made with a Hamilton syringe.

In the case of the reinjection study, the cut taken from the eluting peak was routed into an injection valve with a 2.5-mL loop. Once the loop was filled, the valve was closed and bypassed until pure solvent was emerging from the column. At this point the valve was switched to connect the loop to the channel inlet, thus emptying its contents back into the channel. During the feed of this large sample volume, the field was increased to a ΔT of 50 °C in order to concentrate the polymer at the head of the channel.[30] After completion of the feed cycle, the channel inlet was again switched to the solvent source. The flow was stopped as the ΔT was allowed to return to the original level of 13 °C.

In all experiments the channel effluent was monitored by an Altex UV detector Model 153 (Beckman Instruments) with a 254-nm light source. The signal was fed to a flatbed recorder of Type BBC Goertz Metrawatt. The elution volume for a given component was taken as the volume associated with its peak

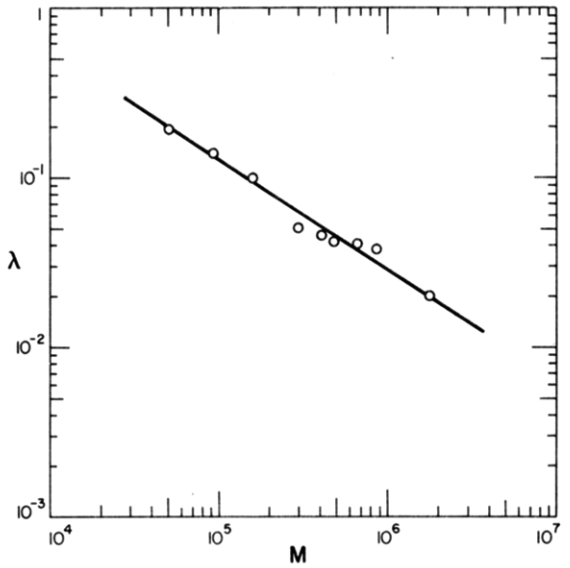

Figure 3. Relationship between retention (as measured by log λ) and molecular weight, plotted according to eq 5, for a set of narrow polystyrene standards analyzed under a constant ΔT of 41 °C at a cold wall temperature of 15 °C. The slope is −0.62 and the correlation coefficient −0.987.

maximum in the recorder tracing.

Results and Discussion

A series of narrow polystyrene standards ranging in molecular weight from 5.1×10^4 to 1.8×10^6 was first studied at a constant temperature drop of 41 °C applied across the channel. By dividing the void volume of the channel by each of the observed elution volumes, a set of retention ratios (R values) was obtained which could be converted graphically into the corresponding set of λ values by the use of Figure 2. According to eq 5 there should exist a linear relationship between log λ and log M whose slope should equal $-b'$, the exponent which relates molecular weight M to the ratio D/D_T. The experimental λ vs. molecular weight relationship is shown in Figure 3. A linear regression analysis of the acquired data gave a value of −0.62 for the slope; the linearity in the data was borne out by a correlation coefficient of −0.987. As sample molecular weights ranged from 5.1×10^4 to 1.8×10^6, this study gave a satisfying confirmation of eq 6 over a large span (about 40-fold) of molar masses. The carrier in this study was THF; the only previous investigation of the relationship between log λ and log M was with ethylbenzene, which is also a good solvent for this polymer.[20] Although 1.6×10^5 was the largest molecular weight analyzed at that time, the value for the slope, $-b'$, was determined as −0.58, in remarkably good agreement with the value, −0.62, from the current study.

A second and more extended test of the postulated relationship between retention, molecular weight, and temperature drop across the channel involves plotting all retention data collected in this study, including both the set measured on the narrow molecular weight standards shown in Figure 3 and a new set obtained from more polydisperse and higher molecular weight samples. The latter have molecular weight averages up to 20.6×10^6. These polymers were studied at a variety of ΔT's, in part because one must use lower ΔT's to avoid extremely high retention levels for higher M polymers. For such varied data, eq 6 offers a suitable relationship between the three observables λ, ΔT, and M. This is illustrated by Figure 4 in which the product of $\lambda\Delta T$ is graphed vs. M in a log–log plot. A linear regression analysis of the data shown in the figure gives

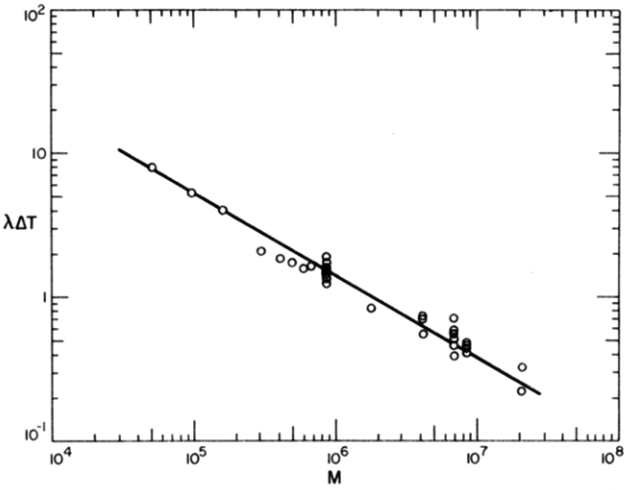

Figure 4. Retention data obtained for a broad range of molecular weights with temperature drops ΔT ranging from 8 to 81 °C and a cold wall temperature of 15 °C. Equation 6 was fit to the data; the slope is −0.53 and the intercept is 3.298.

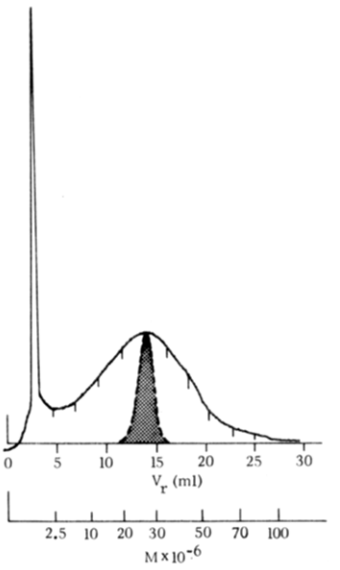

Figure 5. Fractogram of a 20.6×10^6 molecular weight polystyrene obtained at a ΔT of 8 °C. Equations 6 and 7 (the latter corrected for viscosity changes) were used to convert retention volumes into molecular weights. The dotted line represents a peak of a hypothetical monodisperse sample with the peak molecular weight of 23.4×10^6 (as indicated by our data), broadened by nonequilibrium effects only. The nonequilibrium contribution is estimated from the first term on the right in eq 9 using $D = 2.2 \times 10^{-8}$ cm²/s, $\langle v \rangle = 0.0394$ cm/s, and $\chi(\lambda) = 0.545 \times 10^{-3}$.

values of −0.53 for the slope $-b'$ and 3.298 for the intercept; the correlation coefficient was −0.985. Although these coefficients are not identical with those determined for the narrow standards at fixed ΔT, the data show a satisfactory linearity. The discrepancy between the slopes of −0.53 for the complete polymer set (Table I) and −0.62 for the standards is not unexpected in view of the large uncertainties associated with molecular weight assignments made at different laboratories,[31] but it may also reflect some departure from eq 3.

The eluted peak for the polymer of highest molecular weight, 20.6×10^6, is shown in Figure 5. This peak was obtained at $\Delta T = 8$ °C. If we assume that the peak configuration reflects primarily the molecular weight distribution of the polydisperse sample, then the validity of eq 6 justifies the introduction of a molecular weight scale along the elution volume axis. With this addition, Figure

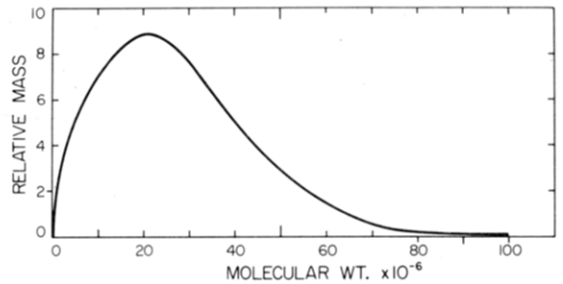

Figure 6. Molecular weight distribution of a polystyrene sample whose manufacturer-assigned molecular weight average is 20.6 × 10^6. The distribution derives from the fractogram in Figure 5.

5 now reflects the molecular weight distribution of the polystyrene sample.

We justify the assumption that the width of the peak is primarily due to the polydispersity of the material by calculating the nonequilibrium peak width, described by the first term on the right of eq 9, which is the primary column contribution to peak broadening.[32] This peak width at the maximum of the observed peak was calculated from the flow rate, channel thickness, sample diffusivity,[33] and retention ratio using eq 9 and previously published relationships.[26] The Gaussian peak corresponding to this estimated band broadening is inserted as a dotted line in the fractogram of Figure 5. Because variances (thus the squares of widths) are additive, nonequilibrium contributes only about 10% of the total plate height. Clearly, most of the peak broadening is due to polydispersity; therefore, the fractogram can be regarded as a molecular weight distribution profile. Multiplication of this profile by the scale correction factor shown in eq 16 yields the unnormalized molecular weight distribution curve plotted in Figure 6.

The molecular weight distribution can be characterized by the sample polydispersity μ, the ratio of weight- to number-average molecular weight, through the use of eq 9 and 10. For the nominal 20.6 × 10^6 molecular weight sample shown in Figure 5, the polydispersity μ is estimated to be 1.52.

As outlined in the Introduction, there is evidence that high molecular weight samples undergo shear degradation during analysis by exclusion chromatography. Such degradation necessarily leads to an underestimation of a polymer's molecular weight, which can be demonstrated by reinjection of a given portion of an elution peak. Where significant shear degradation has occurred, the sample is delayed with respect to its first passage through the SEC column, which indicates transformation into smaller and more penetrating species.

A test for invariant thermal FFF behavior following reinjection was applied to the sample with a molecular weight of 20.6 × 10^6, as seen in Figure 7. This figure, which is a representative of more than ten reinjection runs, confirms that the polymer is indeed separated into fractions upon passage through the thermal FFF system. As expected from the low shear associated with the FFF techniques, there was no significant shift in elution position following reinjection, and thus little apparent degradation.

We conclude that thermal FFF is a gentle fractionation technique, suitable for the characterization of polymeric samples with ultrahigh molecular weights. However, we note that other FFF subtechniques, especially flow FFF and sedimentation FFF, may also work well for such polymers. We have now applied both techniques to nonaqueous systems;[2,4] flow FFF has been specifically applied to linear polystyrenes up to 1.8 × 10^6 molecular weight.[2]

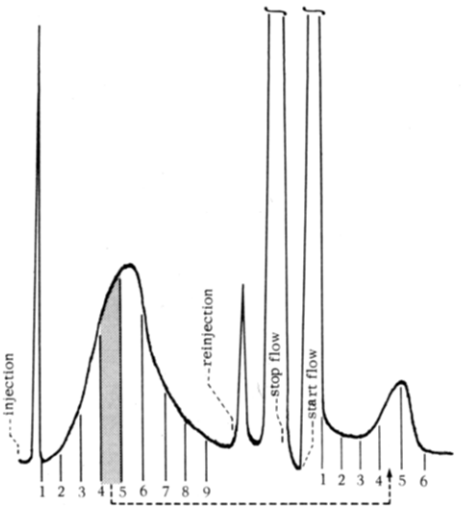

Figure 7. Fractograms of a sample with nominal molecular weight 20.6 × 10^6 obtained at T_c = 13 °C and ΔT = 13 °C. The cross-hatched area in the left fractogram was reinjected into the system as described in the Experimental Section. The reinjected fraction is seen to elute at approximately the same position the second time as it did the first. (The peaks at the start of the reinjection cycle, at the reduction in ΔT from the level of the feed cycle, and at the start of flow are artifacts resulting from the change in operating condition.) The numbered positions refer to the end of a particular fraction. Fractions were collected at constant time intervals; "injection" or "start flow" represents time zero.

Acknowledgment. This work was supported by National Science Foundation Grant CHE-8218503.

References and Notes

(1) J. C. Giddings, M. N. Myers, F. J. F. Yang, and L. K. Smith, "Colloid and Interface Science", M. Kerker, Ed., Academic Press, New York, 1976, Vol. IV, p 381.
(2) S. L. Brimhall, M. N. Myers, K. D. Caldwell, and J. C. Giddings, *J. Polym. Sci., Polym. Lett. Ed.*, **22**, 339 (1984).
(3) J. C. Giddings, G. Karaiskakis, K. D. Caldwell, and M. N. Myers, *J. Colloid Interface Sci.*, **92**, 66 (1983).
(4) K. D. Caldwell, G. Karaiskakis, M. N. Myers, and J. C. Giddings, *J. Pharm. Sci.*, **70** (12), 1350 (1981).
(5) J. C. Giddings and M. N. Myers, *Sep. Sci. Technol.*, **13**, 637 (1978).
(6) J. C. Giddings, M. E. Hovingh, and G. H. Thompson, *J. Phys. Chem.*, **74**, 4291 (1970).
(7) J. C. Giddings, M. N. Myers, G. C. Lin, and M. Martin, *J. Chromatogr.*, **142**, 23 (1977).
(8) S. L. Brimhall, M. N. Myers, K. D. Caldwell, and J. C. Giddings, *Sep. Sci. Technol.*, **16**, 671 (1981).
(9) J. J. Kirkland, *J. Chromatogr.*, **125**, 231 (1976).
(10) J. C. Giddings, Y. H. Yoon, and M. N. Myers, *Anal. Chem.* **47**, 126 (1975).
(11) W. W. Yau, J. J. Kirkland, and D. D. Bly, in "Modern Size Exclusion Chromatography", Wiley-Interscience, New York, 1979, pp 225–227.
(12) E. L. Slagowski, L. J. Fetters, and D. McIntyre, *Macromolecules*, **7**, 394 (1974).
(13) Y. Mei-Ling and S. Liang-He, *J. Liquid Chromatogr.*, **5**, 1259 (1982).
(14) G. H. Thompson, M. N. Myers, and J. C. Giddings, *Anal. Chem.*, **41**, 1219 (1969).
(15) M. N. Myers, K. D. Caldwell, and J. C. Giddings, *Sep. Sci.*, **9**, 47 (1974).
(16) J. C. Giddings, L. K. Smith, and M. N. Myers, *Anal. Chem.*, **48**, 1587 (1976).
(17) J. C. Giddings, M. Martin, and M. N. Myers, *J. Chromatogr.*, **158**, 418 (1978).
(18) J. C. Giddings, M. N. Myers, and J. Janca, *J. Chromatogr.*, **186**, 261 (1979).
(19) M. Martin and R. Reynaud, *Anal. Chem.*, **52**, 2293 (1980).
(20) J. C. Giddings, K. D. Caldwell, and M. N. Myers, *Macromolecules*, **9**, 106 (1976).
(21) J. C. Giddings, K. A. Graff, K. D. Caldwell, and M. N. Myers, in *Adv. Chem. Ser.*, **No. 203**, 259 (1983).

(22) J. C. Giddings and K. D. Caldwell, in "Treatise on Analytical Chemistry", P. J. Elving, Ed., Wiley, New York, in press.
(23) M. E. Hovingh, G. H. Thompson, and J. C. Giddings, *Anal. Chem.*, **42**, 195 (1970).
(24) P. J. Flory, "Principles of Polymer Chemistry", Cornell University Press, Ithaca, NY, 1953, Chapter 14, p 595.
(25) J. J. Gunderson, K. D. Caldwell, and J. C. Giddings, *Sep. Sci. Technol.*, **19**, 667 (1984).
(26) M. Martin, M. N. Myers, and J. C. Giddings, *J. Liquid Chromatogr.*, **2**, 147 (1979).
(27) J. C. Giddings, Y. H. Yoon, K. D. Caldwell, M. N. Myers, and M. E. Hovingh, *Sep. Sci.*, **10**, 447 (1975).
(28) F.-S. Yang, K. D. Caldwell, and J. C. Giddings, *J. Colloid Interface Sci.*, **92**, 81 (1983).
(29) J. C. Giddings, M. N. Myers, K. D. Caldwell, and S. R. Fisher, in *Methods Biochem. Anal.*, **26**, 79 (1980).
(30) J. C. Giddings, G. Karaiskakis, and K. D. Caldwell, *Sep. Sci. Technol.*, **16**, 725 (1981).
(31) C. Strazielle and H. Benoit, *Pure Appl. Chem.*, **26**, 451 (1971).
(32) L. K. Smith, M. N. Myers, and J. C. Giddings, *Anal. Chem.*, **49**, 1750 (1977).
(33) W. Mandema and H. Zeldenrust, *Polymer*, 18, 835 (1977).

Spectroscopy and Triplet Photophysical Properties of Poly[*N*-((vinyloxy)carbonyl)carbazole] and Its Monomeric Analogue

Richard D. Burkhart* and Oksik Lee

Department of Chemistry, University of Nevada, Reno, Nevada 89557

Sylvie Boileau† and Sylviane Boivin

College de France, 75231 Paris, France. *Received November 12, 1984*

ABSTRACT: The triplet photophysical properties of poly[*N*-((vinyloxy)carbonyl)carbazole] (PFCZ) and of its monomeric model *N*-carbethoxycarbazole (MFCZ) have been investigated and compared with those of the widely studied poly(*N*-vinylcarbazole) (PVCA). Two distinct triplet excimeric emissions are observed in solid films of PFCZ. Phosphorescence spectra of PFCZ and MFCZ in rigid solutions are essentially the same as observed previously for PVCA and *N*-alkylcarbazoles, respectively. The fluorescence spectrum of PFCZ is significantly blue shifted relative to PVCA and, unlike PVCA, yields a structured emission both in solution and in the solid film state. In frozen solutions at 77 K spectral shifts of O_2-saturated vs. N_2-saturated solutions indicate the presence of a weakly bound singlet excimer. Phosphorescence lifetimes of PFCZ and MFCZ in rigid media are 6.2 and 7.0 s, respectively. The delayed fluorescence lifetime in solid films of PFCZ at 77 K is 3.5 s. The intensity of delayed fluorescence from PFCZ both in rigid solutions and in solid films depends upon the square of the excitation intensity and is thus thought to arise from triplet–triplet annihilation.

Introduction

Vinyl aromatic polymers demonstrate a strong tendency to form singlet excimers and emit fluorescence signals both in solution and in the solid film state which are characterized by a dominant excimeric component.[1] The phosphorescence spectra, on the other hand, generally are totally monomeric in character in solutions or rigid glasses and totally excimeric in character in solid films.[2] No polymer is more strikingly clear-cut in this regard than poly(*N*-vinylcarbazole) (PVCA).

It is easy to rationalize this strong propensity for excimeric emission in terms of relative conformational arrangements of two carbazolyl groups separated by three sp^3-hybridized carbon atoms. In fact, 1,3-di-carbazolylpropane has served as a useful monomeric model in unraveling the complexities of the photophysical processes of PVCA[3,4] and recent work has shown that *meso*- and *rac*-*d*,*l*-2,4-dicarbazolylpentane provide an even better model.[5,6]

In view of the technological importance of PVCA as a photoconductor and since the carbazolyl group is so versatile in its photophysical activity, it is natural to seek generalizations about the characteristics of this activity and several of these have been reported previously. For example, Houben et al.[7] studied fluorescence properties of a variety of carbazolyl-containing polymers, Beck et al.[8] studied singlet exciton trapping in two polymethacrylate esters which contain the carbazolyl group, and several research groups have examined the photophysical properties of PVCA prepared by cationic as well as free-radical polymerization.[9-11]

In the present work it is our purpose to investigate photophysical characteristics of a carbazolyl-containing polymer representing a significant structural departure from those examined to date. Poly[*N*-((vinyloxy)-carbonyl)carbazole] (PFCZ) (structure I) possesses two interesting characteristics which make its investigation a matter of keen interest.

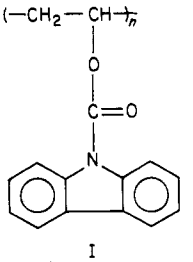

I

In the first place, the carbazolyl group is two atoms removed from the backbone carbon atom and thus enjoys greater steric freedom than it does in PVCA. In addition, and perhaps more importantly, the carbazolyl nitrogen is bonded directly to a carboxylate group having significant electron-withdrawing ability. The effects on luminescence properties of substitution at the nitrogen atom will be seen

† Laboratoire de Chimie Macromoléculaire associé au CNRS, LA 24.

0024-9297/85/2218-1277$01.50/0